JOURNAL OF MATERIALS SCIENCE 18 (1983) 271–277

The interaction of hydrogen and the cementite–ferrite interface in carbon steel

GYE-WON HONG, JAI-YOUNG LEE
Department of Materials Science and Engineering, Korea Advanced Institute of Science and Technology, P.O. Box 150, Cheongyangi, Seoul, Korea

Hydrogen trapping phenomena in carbon steel with controlled amounts of trapping site were studied by permeation experiments. The amount of hydrogen passed through carbon steel membranes was measured by gas chromatography and the diffusivities were calculated from permeation time-lag data. The permeability and diffusivity of hydrogen in carbon steel decrease as the ferrite–cementite interfacial area increases. The trap binding energy of the ferrite–cementite interfaces and hydrogen is calculated to be 10.85 kJ mol^{-1} and the energy level of hydrogen around the trap sites is estimated.

1. Introduction

Hydrogen dissolves in iron exothermically, so large amounts of hydrogen can be supersaturated in iron during heat treatment and this causes hydrogen embrittlement in iron and steel. Hydrogen embrittlement is most serious in high-strength low-alloy steels which are widely used in modern industry. Many theories of hydrogen embrittlement have been suggested, many researchers agree that hydrogen must migrate to a crack-tip area and the hydrogen concentration around the crack tip must exceed a critical value in order to permit crack growth [1–3]. Therefore, the mechanism of hydrogen transport in iron and steel is very important in the understanding of the problem of hydrogen embrittlement.

The published values of hydrogen diffusivity in iron deviate markedly at temperatues below 573 K from the extrapolated values for the high-temperature region. While the apparent activation energy for hydrogen diffusion is in the range 12 to 20 kJ mol^{-1} above 573 K, it lies in the range 36 to 48 kJ mol^{-1} below this temperature. The value extrapolated from the high-temperature region is thus larger than the experimentally measured value. Many researchers believe that these phenomena are due to the trapping of hydrogen in the structural defects (dislocations, microvoids, grain boundaries and interfaces) at low temperatures, as it is energetically favourable for hydrogen to exist in the trap site rather than in the lattice interstitial site [4, 5].

Pressouyre [6] has classified possible trap sites by their physical nature and suggested vacancies, dislocations, alloying element atoms, interfaces and microvoids as possible trapping sites. The actual effective sites have been discussed by many workers: Oriani regards interfaces as the major trapping sites in steels which are not cold worked, with dislocations and microvoids as the major trapping sites in cold-worked steel [7]. Kumnick and Johnson have concluded that dislocations and dislocation debris are the major trapping sites in cold-worked pure ion from permeation measurements [8, 9] whereas Pressouyre found that TiC inclusions are strong irreversible trap sites in steel. Cho *et al.* considered that hydrogen is chemisorbed at grain boundaries in alloyed iron by measuring solubility [10]. It has been suggested by Kotyk and Davis [11] and Newman and Shreir [12, 13] that hydrogen trapping occurs at ferrite–cementite interfaces in carbon steel from the results of diffusivity and solubility measurements on carbon steel. Craig [14] derived the interaction energy of hydrogen and ferrite–ϵ-carbide interfaces as 13.4 kJ mol^{-1}, and Robertson [15] calculated a hydrogen and ferrite–cementite interface energy of 26.8 kJ mol^{-1} from measuring the permeability of hydrogen in AISI 1045 steel. Some researchers claim that methane gas for-

0022–2461/83/010271–07$03.34/0

mation by the reaction $2H_2 + Fe_3C = CH_4 + 3Fe$ in steel is the cause of the abnormal behaviour of hydrogen in iron [16, 17].

All of these researchers failed to isolate the effect of one type of trap site from another because all their experiments were conducted under conditions in which several kinds of trap site existed.

Presently Choo and Lee [18–20] carried out thermal analysis and permeation experiments on pure iron with controlled amounts of one type of trap and obtained the trap activation energy and trap binding energy. They concluded that dislocations or microvoids are dominant trap sites in cold-worked pure iron with respect to their relative density and they estimated the energy level around the dislocations and microvoids. They also applied thermal analysis to carbon steel and obtained a trap activation energy of $13.85\,kJ\,mol^{-1}$ for the ferrite–cementite interfaces.

In this research, hydrogen permeabilities were measured while varying the ferrite–cementite interface area. The trap binding energy of the ferrite–cementite interface was obtained and used to estimate the energy level of hydrogen around the trapping site.

2. Theory

McNabb and Foster [21] have derived an equation which represents the relationship between apparent diffusivity (D_A) and lattice diffusivity (D_L) by considering the variation of lattice dissolved hydrogen concentration and trapped hydrogen concentration separately, assuming that the trapped hydrogen diffuses through the lattice when it escapes from the trapping sites. They have determined the variation of the trapped hydrogen concentration by separately considering the trapping rate (k) and the detrapping rate (p) of hydrogen at trap sites. The equation derived by them is:

$$\frac{a^2}{6D_A} = \frac{a^2}{D_L}\left\{\frac{1}{6} + \frac{\alpha}{2\beta} + \frac{\alpha}{\beta^2} - \frac{\alpha}{\beta^3} \times (1+\beta)\log(1+\beta)\right\}, \quad (1)$$

where a is the specimen dimension, $\alpha = Nk/p$, $\beta = C_0k/p$, N is the trap density and C_0 is the lattice solubility.

Below 673 K, where the amount of trapped hydrogen is much larger than that in lattice sites, $\alpha \gg \beta$, Equation 1 simplifies to:

$$D_L = D_A(1+\alpha). \quad (2)$$

The parameter α can thus be calculated by measuring the apparent diffusivity in conditions where the above criteria are satisfied. If energy levels around the trapping sites are assumed to be those shown in Fig. 1, then the trapping and detrapping rates, k and p, can be written:

$$k = \nu_0 \exp(-E_s/RT) \quad (3)$$

$$p = \nu_1 \exp(-(E_s + E_B)/RT). \quad (4)$$

If it is assumed that the vibration frequencies ν_0 and ν_1 are the same, Equations 5 and 6 are derived:

$$k/p = \exp(E_B/RT) \quad (5)$$

$$\alpha = Nk/p = N\exp(E_B/RT) \quad (6)$$

Since various types of trap site exist in one specimen, it is not possible to measure the effect of a single type of trap site from one kind of specimen. However, the effect of one type of trap site can be obtained from the difference of mean trap parameter (α) of two specimens, which differ only in the amount of single type trap sites that are present. If the amount of one type trap site is different in two specimens, it can be said that the difference of trap parameter (α_2) comes from the effect of the trap site which was varied, and then Equation 7 holds:

$$(D_L/D_{A1}) - (D_L/D_{A2}) = \alpha_2 = \Delta N_i k_i/p_i, \quad (7)$$

where D_{A1} is apparent hydrogen diffusivity in specimen 1, D_{A2} is apparent hydrogen diffusivity in specimen 2 in which the amount of trap site i is varied from specimen 1, ΔN_i is the difference in the number of trap sites i between specimens 1 and 2. Because the trap density does not vary

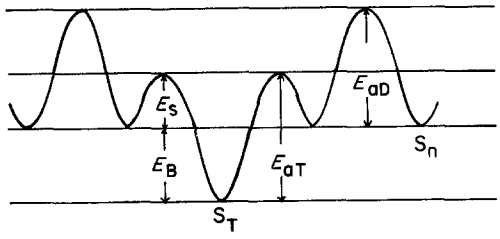

Figure 1 Model for trapping site. E_{aD}, diffusion activation energy of hydrogen in normal lattice; E_s, saddle-point energy; E_B, binding energy between trapping site and hydrogen; E_{aT}, trap activation energy; S_T, trapping site; and S_n, normal lattice site.

TABLE I Chemical composition of the specimens

Specimen	Elements (wt ppm)							
	C	N	S	P	Ni	Cr	Si	Mn
Electrolytic iron	50	–	50	40	–	–	–	50
0.12C carbon steel	1260	50	12	–	411	–	–	–
0.49C carbon steel	4941	58	12	–	509	–	–	–

with temperature, the trap parameter (α_2) obtained at different temperatures for the same specimen can be expressed as Equation 8 by combining Equations 6 and 7. The binding energy of trap site i and hydrogen can be obtained.

$$\alpha_{2_{T_2}}/\alpha_{2_{T_1}} = \exp\left\{\frac{E_B}{R}(1/T_2 - 1/T_1)\right\}. \quad (8)$$

3. Experimental procedure

3.1. Specimen preparation

The materials used in these experiments were the same as those used by Choo [19]. Electrolytic iron and graphite were melted in an induction furnace to make a carbon steel ingot. This ingot was remelted in vacuum arc remelting equipment to remove gas. The chemical compositions of the ingots are shown in Table I. Each ingot was forged and hot-rolled at 1423 K, then normalized for 2 h at 1173 K. Disc-shaped specimens of 40 mm diameter and 0.5 to 0.8 mm thick were cut from this material. Two kinds of carbon steel, 0.12C and 0.49C steel, were used in this work, and their microstructures are shown in Fig. 2.

Both sides of each specimen were ground with emery paper no. 1000 and palladium was electrodeposited on to the surfaces to prevent contamination of the iron. The very high rate of diffusion of hydrogen through palladium, and the extreme thinness of these layers relative to the sample ensured that the palladium did not contribute significantly to the observed permeation kinetics [22].

3.2. Experimental apparatus and procedure

Specimens were mounted in the experimental apparatus as shown in Fig. 3. The specimen surface was activated by raising the temperature above 673 K and charging area L of the reaction chamber with 0.4 MPa hydrogen and passing pure argon into area K. After activating the specimen, the reaction chamber was evacuated to remove the hydrogen dissolved in the specimen and the temperature lowered to the value at which the permeability was to be measured. After temperature equilibration the reaction chamber (L) was filled with hydrogen at constant pressure. The hydrogen passing through the specimen was delivered to the gas chromatograph by argon carrier gas and its amount measured by a thermal conductivity detector. The amount permeating was obtained from the detected value by calibrating the thermal conductivity detector by injecting known amounts of hydrogen in to the gas chromatograph using a gas-tight syringe. The ice trap (I) was used to correct the effect of gas temperature difference on the detected value.

The experiment was continued until the permeation flux reached steady state. After each

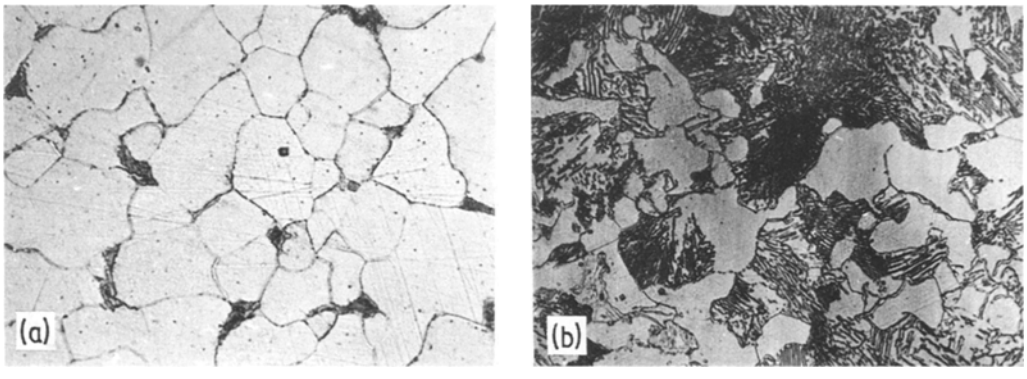

Figure 2 Microstructures of carbon steel. (a) 0.12 wt% carbon steel, (b) 0.49 wt% carbon steel (× 400).

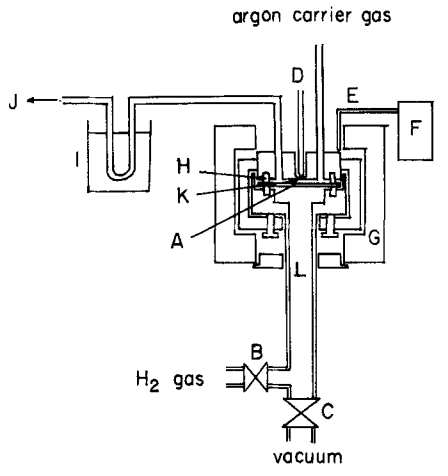

Figure 3 Schematic diagram of hydrogen permeation apparatus. A, specimen; B and C, vacuum needle valve; D, measuring thermocouple; E, controlling thermocouple; F, controller; G, furnace; H, copper O-ring; I, ice trap; J, column (molecular sieve 5A, 2 ft long).

experiment, the specimen was heated above 673 K to remove hydrogen from the specimen. The specimen was then brought to another temperature and the procedure repeated. The experimental temperature range was 400 to 673 K. Apparent diffusivities of hydrogen were calculated from permeation time-lag data (t_i), using the relation $D_{app} = a/6t_i$, where a is the specimen thickness [23].

4. Experimental results and discussion

Hydrogen permeabilities for the 0.12C and 0.49C steel are shown in Fig. 4. Their temperature dependence obtained by the least square method are given in Equations 9 and 10:

$$\Phi_{0.12C} = 1.158 \times 10^{-2} \exp(-43.93\,\text{kJ mol}^{-1}/RT) \quad (9)$$

$$\Phi_{0.49C} = 9.606 \times 10^{-3} \exp(-44.69\,\text{kJ mol}^{-1}/RT) \quad (10)$$

$$[\Phi] = [\text{cm}^3\,(\text{ntp H}_2)\,\text{cm}^{-1}\,\text{sec}^{-1}\,\text{atm}^{-1/2}].$$

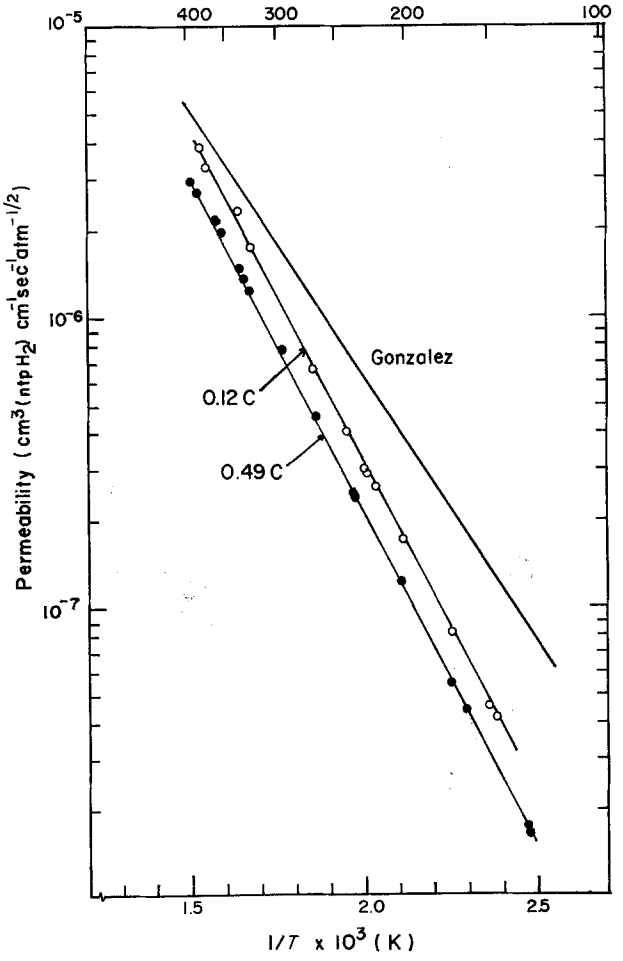

Figure 4 Temperature dependence of hydrogen permeability in carbon steel.

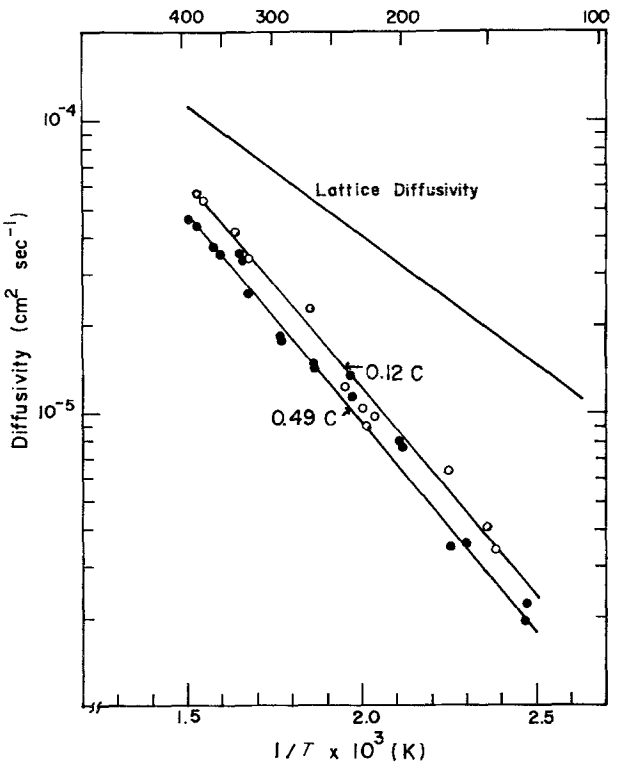

Figure 5 Temperature dependence of apparent hydrogen diffusivity in carbon steel.

The solid line in the figure is that derived by Gonzalez [24]. Our values are smaller than those of Gonzalez, the measured activation energy for permeation is larger than the value obtained by Gonzalez of 35.28 kJ mol^{-1}. Similar results were obtained by Robertson and Thompson for AISI 1045 steel [15]. The decrease of hydrogen permeability with increase of carbon content is thought to be due to the reduced area of ferrite through which easy lattice diffusion is possible.

Fig. 5 shows the apparent hydrogen diffusivities as a function of reciprocal temperature for the 0.12C and 0.49C steel, and their temperature dependences obtained by the least square method are given by Equations 11 and 12:

$$D_{A\,0.12C} = 7.201 \times 10^{-3} \times \exp(-26.79\,\text{kJ mol}^{-1}/RT)\ \text{cm}^2\ \text{sec}^{-1} \quad (11)$$

$$D_{A\,0.49C} = 6.163 \times 10^{-3} \times \exp(-26.94\,\text{kJ mol}^{-1}/RT)\ \text{cm}^2\ \text{sec}^{-1}. \quad (12)$$

The results indicate that hydrogen diffusivity decreases with increase of carbon content as does permeability. This is thought to be caused by hydrogen trapping at the ferrite–cementite interface. The mean trap parameter, α, which represents the effects of all types of trapping site was calculated using Equation 2. In order to obtain α, it is necessary to know D_L. However, reported values of D_L vary and in this work the mean of the reported values [25–28] is used to calculate α:

$$D_L = 2.24 \times 10^{-3} \exp(-16.8\,\text{kJ mol}^{-1}/RT).$$

Calculated values of α are shown in Table II. Because the relative densities of the specimens are 99.94% and 99.95% of theoretical values for the 0.12C and 0.49C steels, respectively, and the specimens were normalized under the same conditions, it is assumed that the number of trapping sites other than at ferrite–cementite interfaces are the same in both steels. The trap parameter, α_2, obtained from the difference of

TABLE II Mean trap parameters (α) in carbon steel

Temperature (K)	α	
	0.12C	0.49C
673	1.8414	2.2119
623	2.1239	2.5569
573	2.5115	3.0314
523	3.0661	3.7129
473	3.9057	4.7468
423	5.2673	6.4314
373	7.6966	9.4532
323	12.6474	15.6545

TABLE III The difference in trap parameters (α_2) between 0.12C and 0.49C carbon steel

Temperature (K)	α_2
673	0.3705
623	0.4330
573	0.5199
523	0.6464
473	0.8411
423	1.1641
373	1.7566
323	3.0071

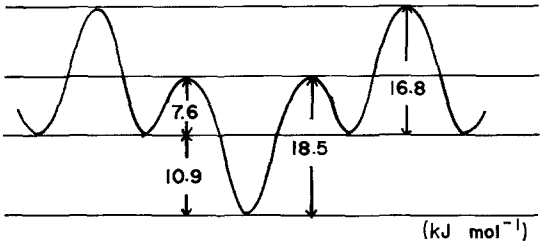

Figure 6 Energy level of hydrogen around the ferrite–cementite interface.

the mean trap parameter, α, describes the effect of the ferrite–cementite interface only and this is presented in Table III. The trap binding energy of ferrite–cementite interfaces and hydrogen calculated from the temperature dependence of α_2 using Equation 8, is $E_B = 10.85\,kJ\,mol^{-1}$.

The value of E_B obtained in this work is smaller than the value obtained by Robertson and Thompson, $26.8\,kJ\,mol^{-1}$ [15]. It is thought that their large value arises because they calculated E_B directly from the temperature dependence of the mean trap parameter, α. The present results are similar to the value obtained by Craig [14] for the trap-binding energy of ϵ-carbide and hydrogen, $13.4\,kJ\,mol^{-1}$. This result indicates that ϵ-carbide–ferrite and ferrite–cementite interfaces have a similar trapping nature, but the ϵ-carbide is slightly more effective for trapping than cementite among the various carbide forms. It is also apparent that the trapping effect of ferrite–cementite interfaces is weaker than that of dislocations or microvoids because the trap binding energy is smaller than the values of dislocations ($26.4\,kJ\,mol^{-1}$) or microvoids ($29.0\,kJ\,mol^{-1}$) obtained by Choo and Lee [19].

The energy levels of hydrogen around ferrite–cementite interfaces are estimated as in Fig. 6, using the present results and the trap activation energy obtained from thermal analysis of the same carbon steel by Choo and Lee [19]. It is found that the saddle-point energy (E_s) is about half the activation energy of normal lattice diffusion.

5. Conclusions

(1) Steady state hydrogen permeation flux in carbon steel decreases as pearlite area increases. The permeabilities are given as follows:

$$\Phi_{0.12C} = 1.158 \times 10^{-2} \exp(-43.93\,kJ\,mol^{-1}/RT) \times [cm^3\,(ntp\,H_2)\,cm^{-1}\,sec^{-1}\,atm^{-1/2}]$$

$$\Phi_{0.49C} = 9.606 \times 10^{-3} \exp(-44.69\,kJ\,mol^{-1}/RT) \times [cm^3\,(ntp\,H_2)\,cm^{-1}\,sec^{-1}\,atm^{-1/2}].$$

(2) The apparent diffusivity of hydrogen in carbon steel decreases as ferrite–cementite interface area increases. The diffusivities are given as follows:

$$D_{A\,0.12C} = 7.201 \times 10^{-3} \times \exp(-26.79\,kJ\,mol^{-1}/RT)\,(cm^2\,sec^{-1})$$

$$D_{A\,0.49C} = 6.163 \times 10^{-3} \times \exp(-26.94\,kJ\,mol^{-1}/RT)\,(cm^2\,sec^{-1}).$$

(3) The trap binding energy of ferrite–cementite interface and hydrogen is measured as $10.85\,kJ\,mol^{-1}$ by isolating only one type of trap site. The energy level of hydrogen around the interfaces is estimated based on this value.

Acknowledgement

The work was supported in part by a grant from the Korea Science and Engineering Foundation.

References

1. J. P. HIRTH, *Met. Trans.* **11A** (1980) 861.
2. I. M. BERNSTEIN and A. W. THOMPSON, *Int. Met. Rev.* **212** (1976) 269.
3. M. CORNET and S. TALBOT-BESNARD, *Met. Sci.* **12** (1978) 335.
4. J. VÖLKL and G. ALEFELD, "Topics on Applied Physics", Vol. 28, "Hydrogen in Metals, 1", edited by G. Alefeld and J. Völkl (Springer-Verlag, Berlin, Heidelberg, New York, 1978) pp. 197–226.
5. R. A. ORIANI, Proceedings of the Conference on Fundamental Aspects of SCC, Ohio State University (1967) edited by R. W. Stoehle (NACE, Houston, 1969) pp. 32–49.
6. G. M. PRESSOUYRE, *Met. Trans.* **10A** (1979) 1571.
7. R. A. ORIANI, *Acta Metall.* **18** (1970) 147.
8. A. J. KUMNICK and H. H. JOHNSON, *Met. Trans.* **5A** (1974) 1199.
9. *Idem, Acta Metall.* **28** (1980) 33.
10. C. G. CHO, J. Y. LEE and W. Y. CHOO, *J. Mater. Sci.* **16** (1981) 1285.

11. M. KOTYK and H. M. DAVIS, *Trans. ASM* **53** (1961) 653.
12. N. F. NEWMAN and L. L. SHREIR, *J. Iron Steel Inst.* **207** (1969) 1369.
13. *Idem, Corrosion Sci.* **11** (1971) 25.
14. B. D. CRAIG, *Acta Metall.* **25** (1979) 1027.
15. W. M. ROBERTSON and A. W. THOMPSON, *Met. Trans.* **11A** (1980) 553.
16. H. H. PODGURSKI, *Trans. AIME* **221** (1961) 389.
17. M. McKIMPSON and P. G. SHEWMAN, *Met. Trans.* **12A** (1981) 825.
18. W. Y. CHOO and J. Y. LEE, *ibid.* **13A** (1982) 135.
19. *Idem, J. Mater. Sci.* **17** (1982) 1930.
20. W. Y. CHOO, PhD thesis, KAIST (1981).
21. A. McNABB and P. K. FOSTER, *Trans. AIME* **227** (1963) 618.
22. A. J. KUMNICK and H. H. JOHNSON, *Met. Trans.* **6A** (1975) 1087.
23. J. CRANK, "The Mathematics of Diffusion" (Clarendon Press, Oxford, 1975).
24. O. D. GONZALEZ, *Trans. AIME* **245** (1969) 607.
25. E. W. JOHNSON and M. L. HILL, *ibid.* **218** (1960) 1104.
26. M. L. HILL and E. W. JOHNSON, *ibid.* **215** (1957) 717.
27. W. BANKOLOH and W. WENZEL, *Arch Eisenhüttenw.* **11** (1937) 273.
28. W. EICHENAUER, H. KUNZIG and A. PEBLER, *Z. Metalkde* **49** (1958) 220.

Received 5 April
and accepted 2 July 1982